LOW STRETCH PMMA BURNING IN MICROGRAVITY: STATUS OF THE GROUND-BASED PROGRAM AND NEW ISS GLOVEBOX EXPERIMENT SALSA

S.L. Olson, NASA Glenn Research Center
J.S. T'ien, CWRU, and
J.B. Armstrong, CWRU

Abstract

The objective of this ground-based program is to study low stretch diffusion flames burning PMMA as the solid fuel to determine the relationship between buoyant low stretch burning in normal gravity and forced flow low stretch burning in microgravity. The low stretch is generated in normal gravity by using the buoyant convection induced by burning the bottom of a large radius of curvature sample. Low stretch is also generated using the Combustion Tunnel drop tower rig (2.2 and 5.2 second facilities), which provides a forced convective low velocity flow past smaller radius of curvature samples . Lastly, an ISS glovebox investigation is being developed to study low stretch burning of PMMA spheres to obtain long duration testing needed to accurately assess the flammability and burning characteristics of the material in microgravity. A comparison of microgravity experiment results with normal gravity test results allows us to establish a direct link between a material's burning characteristics in normal gravity (easily measured) with its burning characteristics in extraterrestrial environments, including microgravity forced convective environments. Theoretical predictions and recent experimental results indicate that it should be possible to understand a material's burning characteristics in the low stretch environment of spacecraft (non-buoyant air movement induced by fans and crew disturbances) by understanding its burning characteristics in an equivalent Earth-based low stretch environment (induced by normal gravity buoyancy). Similarly, Earth-based stretch environments can be made equivalent to those in Lunar- and Martian-surface stretch environments (which would induce partial-gravity buoyancy).

Surface Regression Rates

Figure 1 shows the surface regression rates for PMMA cylinders over the full range of flammability in air, from blowoff at high stretch, to quenching at low stretch, observed for the first time in the normal gravity experiments[1], which are represented by the data circles. Previous higher stretch results[2,3] are represented by the squares and triangles. The solid line drawn through the central portion of the data ($3 < a < 100$ s^{-1}) has a slope of unity, which indicates regression is proportional to stretch. Infinite kinetics theory and experiments find a square root relationship[2] between regression and stretch at high stretch rates. The figure coordinates assume that the values of stretch are equivalent, whether derived from forced stretch or from buoyant stretch. The excellent correlation of the regression-rate data over the two-order-of-magnitude variation of stretch shows the reasonableness of this assumption.
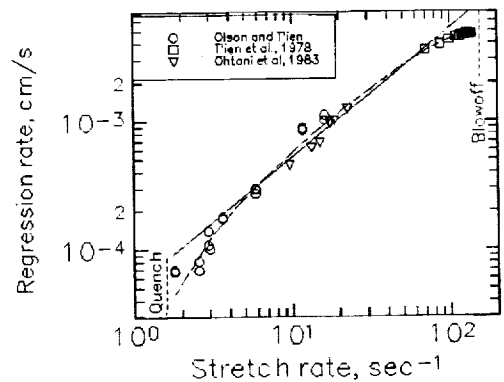
Figure 1: Surface regression rates for PMMA as a function of stretch rate. Data spans from blowoff extinction at high stretch rate to quenching extinction at low stretch rate.

In Figure 1, the stretch rate below which uniform flame burning was not achieved is 3 s^{-1}, where departure from the linear correlation occurs. Flamelets[1] which only partially cover the fuel surface are observed in this region. Similarly, the overall extinction limit is marked simply as a Quench limit, where no flame could be sustained at these large radii (low stretch rates).

Surface Energy Balance

Burning rate data and temperature measurements (gas and solid-phase) were used to evaluate each term of a surface energy balance at the solid surface. To determine overall trends, the terms of the surface balance are compared as ratios as defined below. The ratio $F_{reutilization}$, is the fraction of gas-to-surface net heat flux used to vaporize more fuel, and another ratio, F_{loss}, is the fraction of gas-to-surface net

Figure 2: Loss, Reutilization, and PHI ratios as a function of stretch rate.

heat flux that is lost to the solid interior and radiated from the surface. In this way, $F_{loss}+F_{reutilization}=1$. These ratios are plotted in Fig. 2 as a function of stretch rate. At the Quench limit, only 10% of the heat flux is reused; 90% of it is lost.

PHI, the fraction of gas-to-surface net heat flux that is conducted in depth, is defined for comparison with Yang and T'iens' theory [4]. The flammability of a thick solid is modified considerably by solid-phase heat loss, so the solid phase heat loss is an important additional parameter in experiments with thick solids. The value of PHI at the Quench limit of $a=2$ s^{-1} agrees well with the value of ≈ 0.55 predicted by Yang and T'ien [4] for the same stretch rate in air. It is important to note that over the range of stretch rates studied, that in-depth solid-phase losses are comparable to surface radiative losses, whose strong effect on flammability was shown in Fig.1. Thus for thick fuels, the solid-phase heat loss is expected to be a significant factor in a material's flammability characteristics.

Modeling

A numerical model of the combustion of the solid fuel is being developed concurrently. The theoretical model makes use of an advanced, one-dimensional, gas-phase combustion model implementing a narrow-band radiation model. The gas-phase model is currently being coupled with a transient solid heat conduction model to simulate our drop experiments. The solid model was designed to provide an accurate simulation of the temperature profile within the solid. The transient heat conduction equation with surface regression is:

$$\rho c_s \frac{\delta T}{\delta t} = k_s \frac{\delta^2 T}{\delta x^2} + \rho c_s r \frac{\delta T}{\delta x}$$

where rho represents the density of the solid, c_s represents the local heat capacity, k_s represents the local thermal conductivity (see below), and the regression rate is given as r. The equation was discretized using a Crank-Nicolson scheme to allow for a time-stepping solver to be used. The discretization employed the finite difference method. The solid model is able to respond to rapid changes in incident heat flux and has shown stability at time steps equal to those used by the gas phase model.
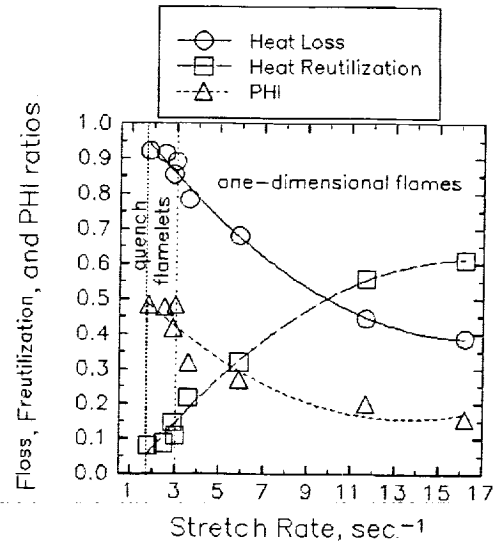
Experiments have shown the formation of bubbles within the plastic, as shown in Figure 3. In order to improve the accuracy of the solid phase model, the heat capacity and thermal conductivities vary with temperature. The thermal conductivity was further modified using a bubble model to correct for the porosity of the burning molten plastic. The bubble model is still under development, but will incorporate bubble nucleation theory and bubble growth dynamics.
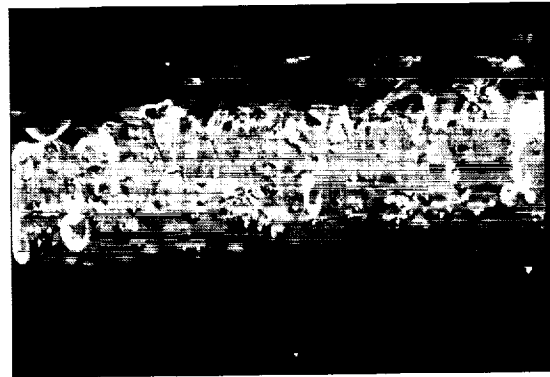
Figure 3: bubble layer in PMMA sample under low stretch burning conditions (1g)

Drop Tower Test Results

Testing is underway using the Combustion Tunnel drop rig, a droppable wind-tunnel capable of low velocity forced flow. The rig has been dropped in both drop towers available at the Glenn Research Center (2.2s and 5.2 s). Cylindrical samples approximately 2 cm in radius are ignited in normal gravity and dropped after stable 1g burning of the sample in air is achieved. The experiment also features the ability to control the rear surface temperature of the PMMA tube. This control over the rear surface is achieved using a combination of a thin heater and a water coolant system. The system may be set to maintain temperature at any value up to 140 deg C.

During an experimental run, data taken include pressures at various points in the flow system to insure proper experiment operation, thermocouples on the front and rear surfaces of the PMMA at the stagnation point to record preheating and surface degradation temperatures, and a heat flux sensor between the rear surface of the PMMA and the inner water coolant system to measure the heat flow from the heated fuel into the central heat sink. Also recorded are two orthogonal video views of the experiment.

Flame standoff distance is very sensitive to the surface energy balance. The flame standoff distance data are shown in Figure 4, and indicate that stable flame standoff distances are obtained for stretch rates above 3 s^{-1}. Preliminary results of microgravity forced stretch gas-phase flame standoff distances agree well with normal gravity buoyant stretch flame standoff distances. However, the limited time available in drop towers do not permit the even the gas-phase to stabilize at very low stretch (<3 sec^{-1}). The solid phase in drop tower experiments has too little time to respond to the g change, and reflects the normal gravity burning heat balance, so these results are qualitative in nature. The microgravity experiments have shown good agreement with the previous 1g tests at similar stretch rates. However, the nature of the experiment requires more time for steady state flames to form in microgravity.
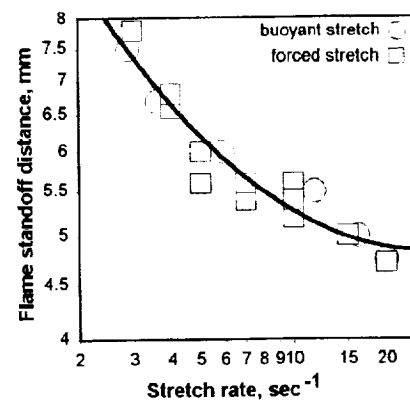
Figure 4::Flame standoff distances for forced and buoyant stretch rates.

Recently published Mir experiments [5] revealed that 4.5 mm diameter cylinders, which were aligned with a low speed concurrent flow (0.5-8 cm/s), burned as low stretch candle-like stagnation flames, as shown in Figure 5, rather than as concurrently spreading flames, which

was the intended configuration. The molten ball of fuel remained at roughly twice the inital radius of the sample, and the flames remained stable to equivalent stretch rates of down to approximately 1.5 sec^{-1}. Oscillating flames were observed prior to extinction at this low stretch rate. Unfortunately, diagnostics were limited to visual images, so detailed energy balances and the quantification of solid phase heat loss, such as those described above for the normal gravity experiments, cannot be made.

Description of the SALSA Investigation in ISS MSG

The SALSA investigation, Solids Aflame in Low Stretch Air, which was recently awarded as an extension of this program, is to study a low stretch flame stabilized at the forward stagnation point of a cast PMMA sphere immersed in a low velocity air flow (Fig. 5). The experiment concept is inspired by recently published results of Mir Skorost experiments[5] where low stretch candle-like flames were obtained. Quantitative temperature measurements of the gas-phase and solid-phase will be obtained, as well as regression rate of the solid sphere.

Figure 5: Color visible image of burning PMMA sphere (1g) with SiC fiber shown extending through the flame zone at the buoyant stagnation point.

The data will be used to make a surface balance for the space experiments, in a manner very similar to the normal gravity data presented above. This data, and numerical modeling of the geometrically-simple experiment, will allow a comparison of the forced and buoyant stretch effects on the heat fluxes balances and flame standoff distances. In addition, the curvature effects will be separated from stretch effects for the small scale flames. Curvature effects on flame standoff distances can be significant compared to the stretch effects for small radii samples. The normal gravity data shown is for large radii cylinders, and provides a baseline set of data with negligible curvature effect. In the proposed experiments, stretch will be varied by varying R as well as U_∞, to provide independent variation of curvature and stretch. Understanding these effects will provide new fundamental information on multidimensional effects on flames.

The experiment requires the use of an infrared camera which will provide a gas-phase SiC fiber temperature and surface temperature field diagnostic. An example IR image is shown in Figure 6, which clearly shows the burning fuel surface and the fiber extending out into the gas phase. The IR camera is narrow-band filtered at 3.8 microns. This diagnostic will provide a much better method of recording the surface temperatures than discrete location thermocouples. The solid thermocouple(s) will provide in-depth heat flux measurements to characterize solid phase heat loss, as well as a temperature reference for emissivity evaluation.

References

[1]Olson, S.L and T'ien, J.S.;*Combustion and Flame*, V. 121, pp. 439-452, 2000.

[2]T'ien, J.S., Singhal, S.N., Harrold, D.P., and Prahl, J.M.; 1978; *Combustion and Flame*, Vol. 33, pp.55-68.

[3]Ohtani, H., Akita, K., and Hirano, T., 1983; *Combustion and Flame*, Vol. 53, pp. 33-40.

[4] Yang, C. T., and T'ien, J.S., 1998, *Journal of Heat Transfer*, Vol. 120, pp. 1055-1063.

[5] Ivanov, A.V, et. al..; NASA Contract NAS3-97160 final report, Russian Space Agency, Keldysh Research Center, Moscow 1999, NASA CP-1999-208917,pp 47-50.
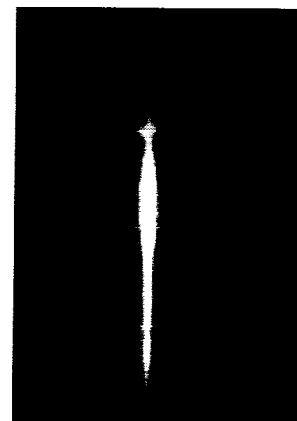
Figure 6: IR image of 1G burning PMMA ball with a SiC fiber extending through the flame zone at the stagnation point.